Minireview

Structure and function in the isolated reaction center complex of Photosystem II: energy and charge transfer dynamics and mechanism

Laurie M. Yoder, Allwyn G. Cole & Roseanne J. Sension*
*Department of Chemistry, University of Michigan, Ann Arbor, MI 48109-1055, USA; *Author for correspondence: (e-mail: rsension@umich.edu)*

Abstract

The dynamics of energy and charge transfer in the Photosystem II reaction center complex is an area of great interest today. These processes occur on a time scale ranging from femtoseconds to tens of picoseconds or longer. Steady-state and ultrafast spectroscopy techniques have provided a great deal of quantitative and qualitative data that have led to varied interpretations and phenomenological models. More recently, microscopic models that identify specific charge separated states have been introduced, and offer more insight into the charge transfer mechanism. The structure and energetics of PS II reaction centers are reviewed, emphasizing the effects on the dynamics of the initial charge transfer.

Abbreviations: 3PEPS – 3 pulse photon echo peak shift; Bchl – bacteriochlorophyll; BRC – bacterial reaction center from purple bacteria; Chl – chlorophyll *a*; FWHM – full width at half maximum; P – special pair in purple bacterial reaction centers; P680 – primary electron donor in Photosystem II, analogous to P; Pheo – pheophytin a; PS II – Photosystem II; RC – reaction center

Introduction

Oxygenic photosynthesis in cyanobacteria, algae, and higher plants is a key chemical transformation supporting life on earth. The membrane bound pigment-protein complex known as Photosystem II (PS II) performs the initial reaction in oxygenic photosynthesis: the conversion of light energy into a redox pair capable of oxidizing water. Within the complex of proteins comprising PS II, the D1–D2-cytochrome *b*559 reaction center complex (RC) is responsible for the primary photoinitiated charge separation.

It is now well established by biochemical means that the RC complex of PS II contains 6 chlorophyll *a* (Chl) molecules, 1 or 2 *β*-carotene molecules, and 2 pheophytin *a* (Pheo) molecules (Kobayashi et al. 1990; Eijckelhoff and Dekker 1995). The physical arrangement, electronic structure and mechanistic roles for these pigments have been the subject of a multitude of biochemical, spectroscopic, and theoretical investigations (Diner and Babcock 1996; Dekker and van Grondelle 2000; Greenfield and Wasielewski 1996; van Grondelle et al. 1994). In particular, the spectroscopically identified P680 primary electron donor has been examined extensively. One can find elsewhere data and analyses that support a monomeric (Rutherford 1986; van Mieghem et al. 1991; van der Vos et al. 1992), dimeric (Kwa et al. 1994a; Noguchi et al. 1998; van Kan et al. 1990) or multimeric (Durrant et al. 1995b; Greenfield et al. 1999) electronic structure for P680. In general, P680 is thought to be analogous to the 'special pair' in purple bacteria, although it has been hypothesized that it is comprised of one 'special pair' Chl and one accessory Chl (van Gorkom 1995; van Gorkom and Schelvis 1993).

The recent advent of a low-resolution crystal structure for PS II isolated from *Synechococcus elongatus* (Zouni et al. 2001) has confirmed the pigment content
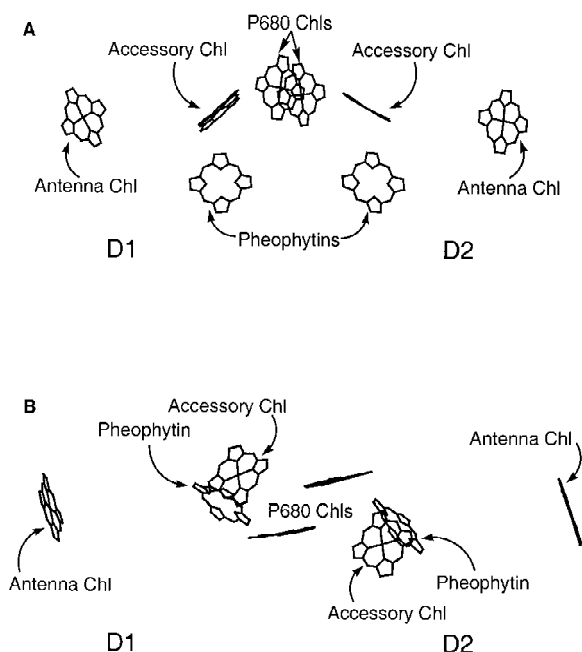
Figure 1. Crystal structure of the PS II reaction center from Zouni et al. (2001). The Chls are represented as porphyrins to illustrate their planar orientations and relative separations; the resolution is insufficient to determine the orientations of the Chl transition dipoles. (A) View along the membrane plane. (B) View onto membrane plane.
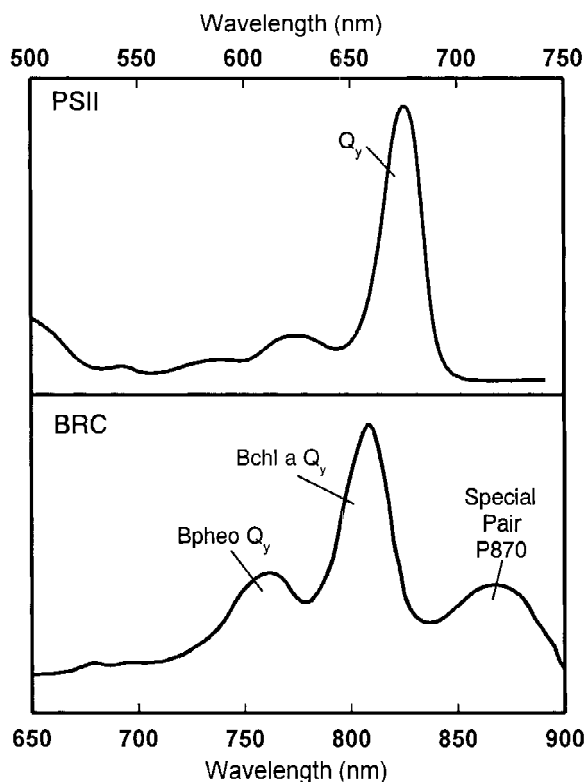

Figure 2. Absorption spectra of PS II (upper) and *R. sphaeroides* bacterial reaction center (lower), showing the overlapping Q_y bands of PS II at 660 to 690 nm compared to the distinct special pair absorption in BRC at ca. 870 nm.

and provided new constraints, limiting the range of possible interpretations for the spectroscopic and kinetic data. However, this structure, shown in Figure 1, reveals the interpigment distances and the orientations of the pigment planes, but not the orientations of the transition dipoles. Without a high-resolution structure defining the orientation and positions of the pigments with angstrom resolution, the methods and data available provide only for indirect rather than direct elucidation of P680 and the mechanism of charge transfer. Thus, the mechanism of charge separation remains an open subject for investigation.

In this Minireview we will summarize the current state of knowledge of the spectroscopic, structural, and kinetic properties of the PS II reaction center, and explore the models proposed for the reaction center mechanism in the light of the available data.

Steady-state spectroscopy of PS II

The interpretation of both steady state and time-resolved spectroscopic studies of PS II is complicated by the strong overlap of the spectra of all RC pigments as shown in Figure 2. At room temperature the Q_y

spectra of Chl and Pheo in solution have bandwidths comparable to the bandwidth of the Q_y transition of the RC ($\Delta\lambda_{Chl,Pheo} \cong 18$ nm (ca. $400\,cm^{-1}$), $\Delta\lambda_{RC} \cong 25$ nm (ca. $550\,cm^{-1}$)). Thus, it is difficult to separate the contributions of individual molecules or excitonic states and investigate their roles in energy and electron transfer in the RC of PS II.

The situation improves somewhat under low-temperature conditions (< 77 K). The widths of the individual bands decrease while the overall RC band width remains broad. Under these conditions the Q_y bands of RC pigments are partially resolved (Konermann and Holzwarth 1996; van Kan et al. 1990). This allows one to distinguish the presence of short-wavelength Chl having maxima at $\lambda \sim 672$ nm and a long-wavelength form located at $\lambda = 680–683$ nm.

Early assignments of the Q_y band of Pheo were based on the isolated Pheo spectrum (Fragata et al. 1988), since the Q_x band is resolved in the RC (544–545 nm) and can be compared with the Q_x transition in isolated Pheo. Based on this comparison, the Q_y band

is expected to appear at ca. 676 nm (Otte et al. 1992; van Kan et al. 1990). Further investigation has led to reports placing Pheo Q_y peaks at different locations in the RC red band (Chang et al. 1994, 1995; Mimuro et al. 1995; Jankowiak et al. 1999). In general, it is now accepted that the active Pheo absorbs near 680 nm, but there is no consensus on the assignment of the inactive Pheo. In particular, the inactive Pheo Q_y absorption has been reported at 668 nm (Jankowiak et al. 1999), 670 nm (Konermann and Holzwarth 1996; Konermann et al. 1997b; Dedic et al. 2000), 671 nm (Mimuro et al. 1995), 672 to 674 nm (Yruela et al. 1999), 676 nm (Germano et al. 2001) and near 680 nm (Shkuropatov et al. 1997).

Notwithstanding the active Pheo absorption near 680 nm, there is reason to believe (Kwa et al. 1992, 1994b; Satoh 1993; Seibert 1993; van Grondelle et al. 1994; Diner and Babcock 1996) that pump wavelengths on the red edge of the Q_y band preferentially excite the Chl of the primary electron donor, P680. One study, however, presents evidence that the P680 transition is near 672 nm (Diner et al. 2001). The red edge absorption near 683 to 684 nm has been the subject of numerous studies. Several groups have attributed this band to the accessory Chl_1 (Konermann et al. 1997b; Germano et al. 2001; Diner et al. 2001). It has also been postulated that a loosely coupled Chl pigment may contribute to the red edge absorption in many preparations of the PS II RC complex. The loosely coupled Chl molecules associated with the core complex interact only weakly with the six central pigments, thus their influence on the energy levels is negligible. The loosely coupled Chl proposed to absorb at 683 to 684 nm has been identified as an energy transfer link between the antenna complex and the reaction center (Chang et al. 1994, 1995), and as one of the peripheral antenna Chls (Finzi et al. 1998, 1999; Jankowiak et al. 1999). Other groups have assigned peripheral antenna absorptions to the blue side, at 670 nm (Schelvis et al. 1994; Vacha et al. 1995; Germano et al. 2001).

Pigment structure in PS II

The pigment structure in the PS II reaction center complex is illustrated in Figure 1. Within the 3.8–4.2 Å resolution of the crystal structure, the coordinates of the pigments of the reaction center have been tentatively assigned (Zouni et al. 2001). However, the orientations of the transition dipoles are not determined in the crystal structure. Thus the crystal structure provides a constraint, but not a determination of the functional structure for energy transfer and charge separation.

In the absence of a high-resolution crystal structure for PS II, additional insight into the reaction center may be obtained from the reaction center structures of purple bacteria. In fact, sequence homology and functional analogies between PS II and the bacterial reaction center (BRC) have led many investigators to use the BRC structure to model PS II (Deisenhofer et al. 1985; Durrant et al. 1995b; Svensson et al. 1996). In contrast to PS II, high-resolution crystal structures have been reported for several different reaction centers from purple bacteria (Deisenhofer et al. 1985, 1995; Yeates et al. 1988; Ermler et al. 1994; Nogi et al. 2000), allowing accurate determination of pigment locations and orientations.

Despite the structural and functional similarities, a critical difference between PS II and BRC is evident in their spectra, as illustrated in Figure 2. In all of the bacterial reaction centers, site energy shifts and strong excitonic coupling between the special pair of bacteriochlorophyll (Bchl) combine to lead to a low-lying absorption band, well isolated from the other pigment transitions. In *Rhodobacter sphaeroides* this absorption band is located at ca. 870 nm. In PS II, on the other hand, the spectrum is highly congested and there is no evidence for a 'special pair' of chlorophyll, with a trap state energetically isolated from the other pigments.

To first order, the special pair of BChl in the BRC can be considered as a dimer of identical chromophores. Assuming point-dipoles, the excitonic interaction energy is given by (see for example van Amerongen et al. 2000, Chapter 2):

$$V_{12} = \frac{\mathbf{D}_{oa}^2 \chi}{R^3} \tag{1}$$

In this equation, $\mathbf{D}_{oa}$ is the dipole transition strength for the Q_y transition of a chlorophyll monomer, $\mathbf{R}$ is the vector connecting the centers of the two chlorophyll monomers, having magnitude $R = |\mathbf{R}|$ and direction $\mathbf{r} = \mathbf{R}/|\mathbf{R}|$, and χ is an orientation factor:

$$\chi = (\mu_1 \cdot \mu_2) - 3(\mathbf{r} \cdot \mu_1)(\mathbf{r} \cdot \mu_2) \tag{2}$$

where μ_1 and μ_2 are the normalized transition dipole moment directions for the two chlorophylls. The parameters for *Blastochloris* (formerly *Rhodopsuedomonas*) *viridis* are $R = 7.6$ Å and $\chi = 1.26$ (Deisenhofer et al. 1985, 1995) and an *in vitro* dipole strength 51 $\mathbf{D}^2$

(BChl *b*) (Scherz and Rosenbach-Belkin 1988). The latter value corresponds to an *in vacuo* value of about 61 $\mathbf{D}^2$ for a refractive index $n = 1.34$ (see the correction factor in Shipman 1977). Thus, the interaction energy in *B. viridis* is $V_{12} = 740–880$ cm^{-1} with an excitonic splitting of $2V_{12} = 1480–1760$ cm^{-1}. The analogous data for *R. sphaeroides* (Ermler et al. 1994), with a special pair of BChl *a*, are $R = 8$ Å, $\chi = 1.07$ and 33–39 $\mathbf{D}^2$ *in vitro* (Shipman 1977; Scherz and Rosenbach-Belkin 1988) (or about 40–48 $\mathbf{D}^2$ *in vacuo*). This yields an interaction energy $V_{12} = 350–500$ cm^{-1} and an excitonic splitting of $2V_{12} = 700–1000$ cm^{-1}. The calculated values of V_{12} are in good agreement with the experimentally measured splittings of *ca.* 1500–1700 cm^{-1} in *B. viridis* and ca. 700–800 cm^{-1} in *R. sphaeroides* (den Blanken and Hoff 1982; Knapp et al. 1985; Scherer and Fischer 1987; Reddy et al. 1993).

In PS II the pigments are Chl *a* with a monomer dipole strength of 17 $\mathbf{D}^2$ (*in vitro*) and 21–23 $\mathbf{D}^2$ (*in vacuo*) (Shipman 1977; Scherz and Rosenbach-Belkin 1988). For geometric parameters analogous to *B. viridis* or *Rb. sphaeroides* the interaction energy in PS II is predicted to be $V_{12} = 245–332$ cm^{-1} or $V_{12} = 179–242$ cm^{-1}, respectively. These values imply excitonic splittings of $360 – 660$ cm^{-1} and are inconsistent with observations in PS II. To account for the decreased coupling between chlorophyll pigments, structural models for PS II based on the BRC have arbitrarily lengthened the separation between the pigments analogous to the bacterial special pair (Chang et al. 1994; Bosch et al. 1995; Durrant et al. 1995b; Svensson et al. 1996). The structure reported by Zouni et al. (2001), in Figure 1, supports this assumption and provides a center-to-center distance of ca. 10 Å. As a consequence of the reduction in 'special pair' coupling in PS II, the couplings between all of the core pigments are comparable in magnitude. This leads naturally to a multimer model for PS II (Durrant et al. 1995b).

Finally, it should also be noted that an alternative structural model for PS II, based on the 3.8 Å resolution crystal structure, was recently published (Vasil'ev et al. 2001). This model predicts a pigment separation of 8.3 Å, and an excitonic coupling of ca. 370 cm^{-1}, effectively introducing a special pair into PS II. This model is not consistent with the spectral data for PS II as described above.

Ultrafast spectroscopic studies of PS II

Ultrafast time-resolved spectroscopies have been applied extensively to the investigation of photosynthetic systems in general, including PS II. Over the last decade many picosecond and femtosecond transient absorption and fluorescence studies have been published investigating the primary charge separation event in PS II. Results reported prior to 1996 are summarized in a review by Greenfield and Wasielewski (1996). The common feature in all of these studies is a wavelength dependent, multiexponential evolution of the spectrum and the excited state and photoproduct populations. Time constants range over four orders of magnitude, from ca. 100 fs to ca. 1 ns.

The recent transient absorption studies have expanded the range of pump and probe wavelengths and have revealed details of the temperature dependence. In emission experiments, a streak camera has been used to achieve an instrumental response function of 4.5 ps (Donovan et al. 1997), which is significantly narrower than the inherent resolution of single photon counting (ca. 30 ps; Gatzen et al. 1996; Konermann et al. 1997a). Even narrower sub-picosecond resolution can be obtained with fluorescence up-conversion, as demonstrated in a preliminary report (Kumazaki et al. 1995), but this technique is susceptible to complications due to multiply excited reaction centers from the necessary high photon flux. In addition, a photon echo experiment has been reported (Prokhorenko and Holzwarth 2000). Recent ultrafast studies not considered in the review of Greenfield and Wasielewski (1996) are summarized in Table 1.

The prevailing interpretation of the kinetic results seems to be that the electronic energy is equilibrated among the six central pigments of the reaction center on a sub-picosecond time scale. It is followed by charge separation with an intrinsic rate of (ca. 1 to 3 ps)$^{-1}$. Some observed components in the 10–50 ps range have been attributed to charge transfer following slow energy transfer from the weakly coupled antenna chlorophylls. Other long time constants are attributed to radical pair relaxation, due to either structural relaxation of the protein matrix or decay to different radical pair states.

Site-directed mutants in PS II

A number of recent studies have compared mutant reaction centers with their analogous wild types, to

Table 1. Summary of ultrafast kinetic studies of PS II

Reference	Method[a]	Excitation (nm)	Probe (nm)	T (K)	Energy transfer[b] (ps)	Intrinsic charge transfer (ps)	Slow energy & charge transfer[c] (ps)	Radical pair relaxation (ps)
(Muller et al. 1996)	TA	680/670	535–555 660–760	277	< 1	2.4	8.9, 19.8	56
(Merry et al. 1996)	TA	665, 680, 694	660–760	ca. 283	0.1, 0.6	3, 21		
(Groot et al. 1997)	TA	685	655–700	20–240		0.4–2.6	18–120	
(Greenfield et al. 1997)	TA	687	543, 558	278		≤ 8	50	
(Greenfield et al. 1999)	TA	661, 683	543.5, 558.5	ca. 7	< 1	5		
(Gatzen et al. 1996)	TRF	620–689	660–690	ca. 277		3	6–30	50
(Donovan et al. 1997)	TRF	656–690	670–694	277		ca. 1	20	
(Konermann et al. 1997)	TRF	650	675–690	77	< 1	1.4		50 – 1 ns
(Kumazaki et al. 1995)	FU	690	730			3, 21		
(Prokhorenko and) Holzwarth 2000)	2PE	674–688		1.3	ca. 100 fs	1.5		25

[a] TA – transient absorption; TRF – time-resolved fluorescence; FU – fluorescence upconversion; 2PE – 2 pulse photon echo.

[b] Energy equilibriation within the central core of RC pigments.

[c] Charge separation that is limited by the energy transfer rate from weakly coupled pigments.

gain further understanding into wild type structure and function. By altering specific protein residues, the binding characteristics of individual pigments can be altered. Specifically, spectroscopic and kinetic studies of isolated PS II reaction centers have employed mutants of *Synechocystis* sp. PCC 6803 and *Chlamydomonas reinhardtii*, with mutations at several different sites: D1-Gln130, which binds the active Pheo; D1-His198 and D2-His197, which bind P680; D1-His118 and D2-His117, which bind peripheral antenna Chls; and D2-Leu205, which is thought to interact with all D1 branch pigments. The main results of these studies are summarized here.

In a first study of the kinetics of mutant reaction centers, Giorgi et al. (1996) employed transient absorption to investigate *Synechosystis* D1-Gln130 mutants. They reported that charge separation in the mutant proceeds with the same time constant as the wild type, but with a varying yield of radical pairs. Subsequent studies by the same group on *Synechosystis* D1-Gln130 and D1-His198 mutants gave similar results: radical yields are affected by mutations near P680 and the active Pheo (Durrant et al. 1998; Merry et al. 1998). The authors concluded that the mutations effectively alter the relative energetics of the charge separated states, and that the radical pair yields are sensitive to fluctuations in the energetics (Merry et al. 1998). In time resolved studies of *C. reinhardtii*, D2-Leu205 mutants exhibited slower charge transfer kinetics than the wild type (Andronis et al. 1999). This experiment showed that the differing identities of the particular residue at D2-205 and the corresponding location in BRC do not account for the different charge separation dynamics between BRC and PS II.

Other time-resolved mutant studies have focused on D2-His117 and D1-His118 in *Synechocystis* (Vasil'ev and Bruce 2000) and *C. reinhardtii* (Johnston et al. 2000). Both groups found that the mutations affect the kinetic component attributed to charge separation following slow energy transfer, providing further evidence that the weakly coupled peripheral antenna chlorophylls are involved in this process.

Spectroscopic studies of *Synechocystis* mutants have led to further understanding of the identities of wild-type pigment transitions. Stewart et al. (2000) identified transitions for the Pheos, P680, and Chl_1 (the accessory chl on D1) that are in keeping with the previously mentioned wild type data. Diner et al. (2001) have reported that D1-His198 and D2-His197 mutations affect the reduction potential of P680, and have identified the accessory chlorophyll, Chl_1, as giving rise to a red-absorbing transition (684 nm). They propose, based on these results, that Chl_1 is the primary electron donor at low temperatures.

Mechanism and models of energy and charge transfer

The detailed mechanism of energy and charge transfer in PS II reaction centers has long been an issue of discussion. Definitive answers have been elusive, in part because of the extensive spectral overlap among the pigment absorptions and the lack of a crystal structure at atomic resolution as discussed above. In models of PS II dynamics based on time resolved experimental data, the kinetics have typically been fitted with sums of exponential decays, with each component assigned to energy or charge transfer. The approach of fitting data to multiple exponentials, while providing a convenient means of representing the data, has limited ability to reveal the details of the microscopic process. Many fitting parameters are obtained, but their physical interpretation is unclear and often speculative. Indeed, in a disordered system with divergent kinetics (such as PS II), one would expect a simple exponential decay model to be inadequate. To more accurately represent the disordered reaction center environment, several groups have performed data analyses by fitting with a distribution of rate constants (Govindjee et al. 1990; Konermann et al. 1997a; Johnston et al. 2000). This method provides a more robust fitting algorithm, and its intuitive interpretation is appealing. However, the same uncertainties associated with assigning the fitted time constants remain.

Recent experimental and theoretical efforts have begun to go beyond phenomenological models to elucidate the microscopic details of energy and charge transfer in PS II. In a first step toward this end, Durrant et al. (1995b) introduced the multimer model for energy transfer, which showed that the excitation energy in the reaction center could be delocalized over multiple pigments. This model is supported by experimental evidence that the initially excited state is delocalized (Greenfield et al. 1999), and that the first charge transfer step proceeds from a delocalized electronic state (Peterman et al. 1998). Spectroscopic investigations of reaction centers with modified pheophytin composition have also indicated the importance of excitonic delocalization, with the additional insight that excitonic interactions are more pronounced on the active branch than on the inactive branch (Germano et al. 2001).

Microscopic models of the charge transfer steps in PS II, to a first approximation, can be based on the analogous process in bacterial reaction centers (Kirmaier and Holten 1993). The main route of charge separation in bacterial systems begins with energy transfer to the special pair (P), which donates an electron to the accessory bacteriochlorophyll (Bchl a) to form P^+Bchl a^-. This state subsequently decays to $P^+H_A^-$ where H_A is the bacteriopheophytin on the L branch. This charge separation is completed on a time scale of ca. 3 ps. In PS II, there is no special pair to trap the excitation energy, but the comparable model is given by:

$$P680^* \, Chl_1 Pheo_1 \rightarrow P680^+ Chl_1^- Pheo_1$$
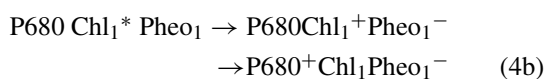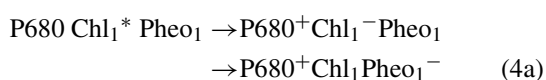$$\rightarrow P680^+ Chl_1 Pheo_1^- \qquad (3)$$
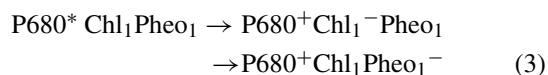
where P680 is the PS II analogue of P, Chl_1 is the accessory chlorophyll on D1, and $Pheo_1$ is the pheophytin on D1. The electronic excitation is indicated by (*). Experimental evidence has been presented for the existence of a chlorophyll anion state, such as the intermediate state in Equation (1) (Durrant et al. 1998). The relative free energy of this state has not been measured, but quantum chemical calculations indicate that it is nearly isoenergetic with the excited singlet state (Blomberg et al. 1998). The final charge separated state ($P680^+Pheo_1^-$) has been estimated to lie below the excited singlet state by 160–950 cm^{-1}, based on recombination fluorescence studies (Booth et al. 1990; Roelofs et al. 1991; Volk et al. 1993; Groot et al. 1994). Quantum calculations place this state at nearly the same energy as both the excited singlet state and the intermediate charge separated state (Blomberg et al. 1998). The low driving force for charge separation has been implicated as a possible cause for the relatively slow charge separation kinetics compared with that of bacterial reaction centers (Dekker and van Grondelle 2000).

Recently, we have developed a microscopic model that describes energy and charge transfer in room temperature PS II using the charge separation scheme similar to Equation (3) (J.J. Shiang, L. M. Yoder and R. J. Sension, submitted for publication). In this model, the excited singlet states and charge transfer states are coupled with a protein matrix, and the master equation is solved to determine the time dependence of charge transfer. The energetics of the excitonic states are based on the multimer model (Durrant et al. 1995b), and the charge transfer couplings are derived from *ab initio* calculations of bacterial reaction centers (Zhang and Friesner 1998). An advantage of this model over phenomenological curve fitting is that the input parameters are deduced from independent theoretical and experimental work, so their physical meaning is clear. The model accurately simulates the

experimentally observed emission kinetics and their wavelength dependence.

Other possible locations of the charges and the excitation energy must also be considered in a more complete model. Several minor energy and charge transfer pathways have been identified in BRC; they involve excitation and a cation localized on the accessory bacteriochlorophyll (van Brederode and van Grondelle 1999). Recent studies have demonstrated that such a channel may be important in PS II as well. Diner et al. (2001) propose a mechanism for charge separation based on their spectral study of PS II mutants. They do not include excitonic coupling in their analysis, thus the donor state is not delocalized, but attributed to a specific pigment, the accessory chlorophyll. At low temperature the mechanism is proposed to be:

$$P680\ Chl_1{}^*\ Pheo_1 \rightarrow P680^+Chl_1{}^-Pheo_1$$
$$\rightarrow P680^+Chl_1Pheo_1{}^- \qquad (4a)$$

$$P680\ Chl_1{}^*\ Pheo_1 \rightarrow P680Chl_1{}^+Pheo_1{}^-$$
$$\rightarrow P680^+Chl_1Pheo_1{}^- \qquad (4b)$$

Charge separation proceeds by two possible intermediate states, which likely have similar energetics. Diner et al. (2001) also note that at room temperature the traditional mechanism (Equation (3)) is also expected to occur, although the mechanism in Equations (4a) and (4b) is three times more likely. A similar model has been proposed by Prokhorenko and Holzwarth (2000) to explain their photon echo experimental results at low temperature. Their model accounts for both energy and charge transfer observed in the dephasing of the initially excited state, and in low temperature transient absorption experiments:

$$(RC\ core)^{*'} \rightarrow (RC\ core)^* \rightarrow P680\ Chl_1{}^+Pheo_1{}^-$$
$$\rightarrow P680^+Chl_1Pheo_1{}^- \qquad (5)$$
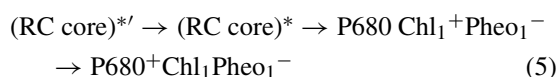
In this scheme the pigments are excitonically coupled so that the initially excited state $(RC\ core)^{*'}$ becomes delocalized over the reaction center $(RC\ core)^*$ in 100–500 fs. The intermediate charge transfer state, formed with an intrinsic rate constant of ca. 1.5 ps, is attributed uniquely to $Chl_1{}^+Pheo_1{}^-$. These charge transfer mechanisms are illustrated in Figure 3.

From these studies, it appears that multiple charge transfer pathways are possible in PS II and detailed microscopic models should account for them. Models of fluorescence may not be able to distinguish between different intermediate radical pair states, since these states do not emit; thus our model as described above succeeds for fluorescence simulations with a single intermediate state. However, extension of such a model to simulate transient absorption may require inclusion of the $Chl_1{}^+Pheo_1{}^-$ state.

Static disorder

The spectroscopic line width for transitions to the singlet excited state in PS II has contributions from both homogeneous and inhomogeneous broadening. Homogeneous broadening results from the coupling of the electronic transition to intramolecular vibrations of the chromophore and the coupling to lattice vibrations (phonons) associated with the protein matrix. The degree of coupling depends on the thermal populations of the coupled vibrations, thus homogeneous broadening is highly temperature dependent. Inhomogeneous broadening results from static disorder in the electronic energy of the transition due to the specific random protein environment, and is generally assumed to be temperature independent. The total width of the transition (FWHM) is given by $\Gamma^2 = \Gamma_{inh}{}^2 + \Gamma_{hom}{}^2$ where Γ_{inh} and Γ_{hom} are the FWHM of the inhomogeneous and homogeneous components, respectively (van Amerongen et al. 2000, Chap. 5). Spectral investigations of PS II over a wide temperature range have shown that at room temperature the linewidth is dominated by homogeneous broadening (Cattaneo et al. 1995; Konermann and Holzwarth 1996). Values of Γ_{hom} at room temperature range from 180 cm^{-1} for pheophytin to 324 cm^{-1} for P680 (Cattaneo et al. 1995). Hole burning experiments have consistently shown that the inhomogeneous broadening is on the order of 100 cm^{-1} (Jankowiak et al. 1989; Tang et al. 1990, 1991; Chang et al. 1995).

Microscopic models of energy transfer in the reaction center require consideration of static disorder with varying levels of detail. The total static disorder is comprised of diagonal and off-diagonal disorder. Off-diagonal disorder accounts for variations in the couplings between electronic states. To date, models have neglected off-diagonal disorder. Diagonal disorder accounts for static shifts in the energies of the electronic states. Simple diagonal disorder has been included successfully in models of hole burning, transient absorption and emission experiments. Recently, however, with the advent of photon echo experiments, more detailed representations of static disorder have become necessary for modeling the data,
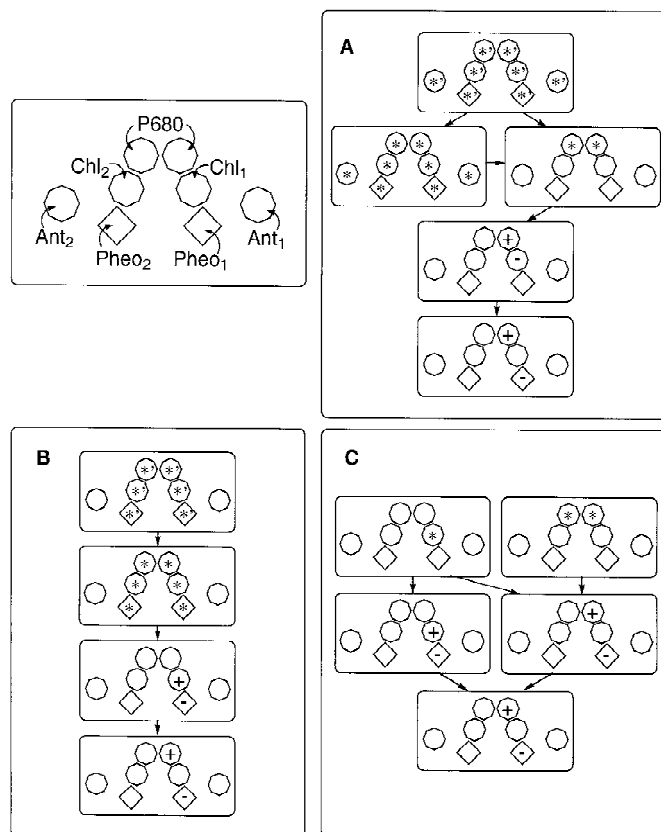
Figure 3. Models for charge transfer. *, initial electronic excitation; *, electronic excitation after energy transfer; + and −, cation and anion. (A) From Shiang, Yoder and Sension, submitted for publication; (B) from Prokhorenko and Holzwarth (2000); (C) from Diner et al. (2001).

including distinguishing between correlated and un-correlated disorder (Yang and Fleming 2000; Agarwal et al. 2001), discussed in more detail below.

The simplest way to incorporate static disorder in a microscopic model of energy transfer is to assume un-correlated Gaussian distributions (with FWHM Γ_{inh}) of site energies distributed around each of the elec-tronic states. This approach is used in the 'multimer' model of energy transfer (Durrant et al. 1995b) and in our energy and charge transfer model (Shiang et al. submitted for publication). The intermolecular coup-lings in PS II are on the order of 20 to 100 cm^{-1}, so Γ_{inh} on the order of 100 cm^{-1} can potentially affect the energy transfer dynamics. Durrant et al. (1995b) found in their numerical simulations that the degree of exciton delocalization weakly depends on the width of the static distribution, for reasonable values of Γ_{inh}. For example, for values of $\Gamma_{inh} \leq$ 200 cm^{-1}, the exciton remains delocalized between 3 to >4 pigments.

As more detailed experimental data become avail-able, more sophisticated ways of accounting for static disorder have become necessary. Recent three pulse photon echo peak shift (3PEPS) studies of B800 in the bacterial light harvesting complex of *R. acidophila* have illustrated the distinction between correlated and uncorrelated disorder (Agarwal et al. 2001; Yang and Fleming 2000). (This technique has not been applied to PS II, but the similarities between bacterial systems and PS II point to the future importance of these ideas for the study of PS II.) In this model, a given reac-tion center has a degree of uncorrelated disorder, σ, between the individual pigments, and all the pigments of that reaction center have a common (correlated) static shift, Σ, relative to other reaction centers of the ensemble. Thus, the total width of the static dis-tribution is $\Gamma_{inh}^2 = \Sigma^2 + \sigma^2$. The 3PEPS technique is able to distinguish correlated from uncorrelated dis-order, with both components contributing significantly in B800 ($\Sigma = 50$ cm^{-1}; $\sigma = 90$ cm^{-1}) (Agarwal et al. 2001).

While experiments have revealed the static disorder of the singlet excited states from hole burning and temperature dependent spectral data, there are no comparable data for charge separated states. However, there is indirect evidence that points to static disorder in the radical pair states as a possible cause of the observed multiexponential kinetics in transient absorption and emission kinetics (Booth et al. 1991; Greenfield and Wasielewski 1996; Groot et al. 1994). Radical pair recombination studies of PS II (Groot et al. 1994) and BRC (Ogrodnik et al. 1994) have been interpreted through models that estimate the static disorder to be on the order of Γ_{inh} = ca. 500–800 cm^{-1}. This estimated disorder is significantly larger than that for the singlet excited states, and it is roughly equal to the estimated ΔG in PS II, where ΔG is the free energy difference between the singlet excited state and the charge separated state, P680$^+$Pheo$^-$. The relatively large energetic width of the charge separated state may result from the corresponding increase in dipole moment, which may make the radical state more sensitive than the neutral excited state to the specific protein arrangement.

Recently, Barter et al. (2001) modeled the multiexponential kinetics of time-resolved fluorescence experiments using a three-step sequential mechanism that relies on the inclusion of significant static disorder. Previously, the same group showed that an analogous two-step model inadequately fit the data (Durrant et al. 1995a). Konermann et al. (1997a) also found that a similar two-step model with a static distribution gave poor agreement with their fluorescence data. In the successful 3-step phenomenological representation (Barter et al. 2001), electron transfer proceeds from an initial donor state to two sequential charge-separated states. The charge separated states have significant static disorder, which is necessary for the model to produce multiexponential kinetic behavior. While able to reproduce the experimentally observed kinetic trends, this model does not provide information on the microscopic identities of the states, nor does it take into account the kinetics of energy transfer between the reaction center pigments.

Because the couplings between electronic states, the variations in site energies and the energetic disorder are all of the same magnitude, a detailed model of the dynamics of PS II must account for all of the above, as in our model (Shiang et al., submitted for publication). We find that the predicted kinetics and radical pair yield depend sensitively on the inhomogeneous width. As the static disorder increases, the
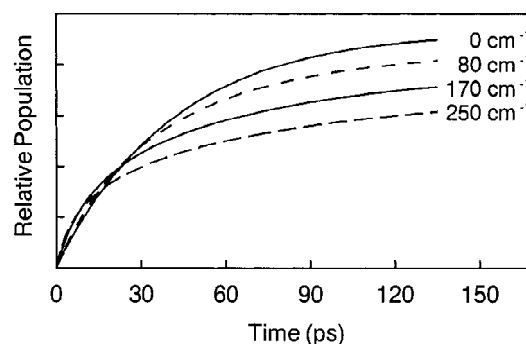

Figure 4. Calculated population kinetics of the P680$^+$Pheo$^-$ radical pair with static disorder from 0 to 250 cm^{-1} (FWHM).

calculated radical pair yield decreases, and the kinetic profile becomes more divergent, giving the appearance of more exponential components, as shown in Figure 4. Clearly, any proposed mechanism or modeling scheme must account for the effects of static disorder.

Conclusions

Ultrafast spectroscopic measurements have identified the key processes of energy and charge transfer in PS II. After excitation of the reaction center, energy is equilibrated within a femtosecond to picosecond time scale. The excited state is likely to be excitonically delocalized over multiple pigments. Charge separation occurs on a picosecond time scale, and longer time components are evident due to the interplay between charge transfer and slower energy transfer from peripheral Chls and the reaction center, as well as interactions with the protein matrix. There is still no consensus, however, on the degree of excitonic delocalization, the specific assignments of the various observed components, or the details of the charge transfer mechanism.

To approach the problem from a theoretical perspective, a high resolution crystal structure is necessary. While there has been recent progress in this area, simulations still rely on the analogous bacterial reaction center structure. To model most accurately the dynamics in PS II, simulations should include multiple charge separated states, like those shown in Figure 3, and take proper account of static disorder in the system. To integrate fully the experimental and theoretical models, progress is needed in several areas: (1) a high-resolution crystal structure; (2) accurate calculations of the relative energies of all charge-separated

states; and (3) wavelength-dependent, subpicosecond experimental results, to test model predictions.

Acknowledgments

References

Agarwal R, Yang M, Xu Q-H and Fleming GR (2001) Three pulse photon echo peak shift study of the B800 band of the LH2 complex of *Rps. acidophila* at room temperature: a coupled master equation and nonlinear optical response function approach. J Phys Chem B 105: 1887–1894

Andronis C, Merry SAP, Durrant JR, Klug DR, Barber J and Nixon PJ (1999) Mutation of the *Chlamydomonas reinhardtii* analogue of residue M210 of the *Rhodobacter sphaeroides* reaction center slows primary electron transfer in Photosystem II. Photosynth Res 62: 205–217

Barter LMC, Bianchietti M, Jeans C, Schilstra MJ, Hankamer B, Diner BA, Barber J, Durrant JR and Klug DR (2001) Relationship between excitation energy transfer, trapping, and antenna size in Photosystem II. Biochemistry 40: 4026–4034

Blomberg MRA, Siegbahn PEM and Babcock GT (1998) Modeling electron transfer in biochemistry: a quantum mechanical study of charge separation in *Rhodobacter sphaeroides* and Photosystem II. J Am Chem Soc 120: 8812–8824

Booth PJ, Crystall B, Giorgi LB, Barber J, Klug DR and Porter G (1990) Thermodynamic properties of D1/D2/cytochrome *b*-559 reaction centres investigated by time-resolved fluorescence measurements. Biochim Biophys Acta 1016: 141–152

Booth PJ, Crystall B, Ahmad I, Barber J, Porter G and Klug DR (1991) Observation of multiple radical pair states in Photosystem 2 reaction centers. Biochemistry 30: 7573–7586

Bosch MK, Proskuryakov II, Gast P and Hoff AJ (1995) Relative orientation of the optical transition dipole and triplet axes of the Photosystem II primary donor. A magnetophotoselection study. J Phys Chem 99: 15310–15316

Cattaneo R, Zucchelli G, Garlaschi FM, Finzi L and Jennings RC (1995) Thermal broadening analysis of absorption spectra of the D1/D2/cytochrome *b*-559 complex in terms of gaussian decomposition sub-bands. Biochemistry 34: 15267–15275

Chang H-C, Jankowiak R, Reddy NRS, Yocum CF, Picorel R, Seibert M and Small GJ (1994) On the question of the chlorophyll a content of the Photosystem II reaction center. J Phys Chem 98: 7725–7735

Chang HC, Small GJ and Jankowiak R (1995) Temperature dependent hole burning of the 684 nm chlorophyll *a* of the isolated reaction center of Photosystem II: confirmation of the linker model. Chem Phys 194: 323–333

Dedic R, Lovcinsky M, Vacha F and Hala J (2000) Low-temperature absorption off-resonant hole-burning spectroscopy of pheophytine a in Photosystem II reaction center. J Luminescence 87-89: 809–811

Deisenhofer J, Epp O, Miki K, Huber R and Michel H (1985) Structure of the protein subunits in the photosynthetic reaction centre of *Rhodopseudomonas viridis* at 3 Å resolution. Nature 218: 618–624

Deisenhofer J, Epp O, Sinning I and Michel H (1995) Crystallographic refinement at 2.3 Å resolution and refined model of the photosynthetic reaction centre from *Rhodopseudomonas viridis*. J Mol Biol 246: 429–457

Dekker JP and van Grondelle R (2000) Primary charge separation in Photosystem II. Photosynth Res 63: 195–208

den Blanken HJ and Hoff AJ (1982) High resolution optical absorption-difference spectra of the triplet state of the primary donor in isolated reaction centers of the photosynthetic bacteria *Rhodopseudomonas sphaeroides* R-26 and *Rhodopsuedomonas viridis* measured with optically detected magnetic resonance at 1.2 K. Biochim Biophys Acta 681: 365–374

Diner BA and Babcock GT (1996) Structure, dynamics, and energy conversion efficiency in Photosystem II. In: Ort DR and Yocum CF (eds) Oxygenic Photosynthesis: The Light Reactions, pp 213–247. Kluwer Academic Publishers, Dordrecht, The Netherlands

Diner BA, Schlodder E, Nixon PJ, Coleman WJ, Rappaport F, Lavergne J, Vermaas WFJ and Chisholm DA (2001) Site-directed mutations at D1-His198 and D2-His197 of Photosystem II in *Synechocystis* PCC 6803: sites of primary charge separation and cation and triplet stabilizations. Biochemistry 40: 9265–9281

Donovan B, Walker II LA, Kaplan D, Bouvier M, Yocum CF and Sension RJ (1997) Structure and function in the isolated reaction center complex of Photosystem II. 1 Ultrafast fluorescence measurements of PS II. J Phys Chem B 101: 5232–5238

Durrant JR, Nixon PJ, Barber J and Klug DR (1998) Identification of chlorophyll anion states during charge separation in mutant Photosystem II reaction centers. In: Garab G (ed) Photosynthesis: Mechanisms and Effects, Vol II, pp 1041–1044. Kluwer Academic Publishers, Dordrecht, The Netherlands

Durrant JR, Porter G, Barber J and Klug DR (1995a) The influence of energy level disorder on the charge separation/trapping kinetics in photosystem II. In: Mathis P (ed) Photosynthesis: From Light to Biosphere, Vol I, pp 611–614. Kluwer Academic Publishers, Dordrecht, The Netherlands

Durrant JR, Klug DR, Kwa SLS, van Grondelle R, Porter G and Dekker JP (1995b) A multimer model for P680, the primary electron donor of Photosystem II. Proc Natl Acad Sci USA 92: 4798–4802

Eijckelhoff C and Dekker JP (1995) Determination of the pigment stoichiometry of the photochemical reaction center of Photosystem II. Biochim Biophys Acta 1231: 21–28

Ermler U, Fritzsch G, Buchanan SK and Michel H (1994) Structure of the photosynthetic reaction centre from *Rhodobacter sphaeroides* at 2.65 Å resolution: cofactors and protein-cofactor interactions. Structure 2: 925–936

Finzi L, Elli G, Zucchelli G, Garlaschi FM and Jennings RC (1998) Long wavelength absorption transitions in the D1/D2/cytochrome *b*-559 complex as revealed by selective pigment photobleaching and circular dichroism measurements. Biochim Biophys Acta 1366: 256–264

Finzi L, Zucchelli G, Garlaschi FM and Jennings RC (1999) Thermal sensitivity of the red absorption tail of the Photosystem II reaction center complex. Biochemistry 38: 10627–10631

Fragata M, Norden B and Kurucsev T (1988) Linear dichroism (250–700 nm) of chlorophyll a and pheophytin a oriented in a lamellar phase of glycerylmonooctanoate/H_2O. Characterization of electronic transitions. Photochem Photobiol 47: 133–143

Gatzen G, Muller Mg, Greibenow K and Holzwarth AR (1996) Primary processes and structure of the Photosystem II reaction center. 3. Kinetic analysis of picosecond energy transfer and charge separation processes in the D1–D2-cyt-b559 complex measured by time-resolved fluorescence. J Phys Chem 100: 7269–7278

Germano M, Shkuropatov AY, Permentier H, de Wijn R, Hoff AJ, Shuvalov VA and van Gorkom HJ (2001) Pigment organization and their interactions in reaction centers of Photosystem II: optical spectroscopy at 6 K of reaction centers with modified pheophytin composition. Biochemistry 40: 11472–11482

Giorgi LB, Nixon PJ, Merry SAP, Joseph DM, Durrant JR, De Las Rivas J, Barber J, Porter G and Klug DR (1996) Comparison of primary charge separation in the Photosystem II reaction center complex isolated from wild-type and D1-130 mutants of the cyanobacterium $Synechocystis$ PCC 6803. J Biol Chem 271: 2093–2101

Govindjee, van de Ven M, Preston C, Seibert M and Gratton E (1990) Chlorophyll a fluorescence lifetime distributions in open and closed Photosystem II reaction center preparations. Biochim Biophys Acta 1015: 173–179

Greenfield SR and Wasielewski MR (1996) Excitation energy transfer and charge separation in the isolated Photosystem II reaction center. Photosynth Res 48: 83–97

Greenfield SR, Seibert M, Govindjee and Wasielewski MR (1997) Direct measurement of the effective rate constant for primary charge separation in isolated Photosystem II reaction centers. J Phys Chem B. 101: 2251–2255

Greenfield SR, Seibert M, Govindjee and Wasielewski MR (1999) Time-resolved absorption changes of the pheophytin Q_x band in isolated Photosystem II reaction centers at 7K: energy transfer and charge separation. J Phys Chem B 103: 8364–8374

Groot M-L, Peterman EJG, van Kan PJM, van Stokkum IHM, Dekker JP and van Grondelle R (1994) Temperature-dependent triplet and fluorescence quantum yields of the Photosystem II reaction center described in a thermodynamic model. Biophys J 67: 318–330

Groot M-L, van Mourik F, Eijckelhoff C, van Stokkum IHM, Dekker JP and van Grondelle R (1997) Charge separation in the reaction center of Photosystem II studied as a function of temperature. Proc Natl Acad Sci USA 94: 4389–4394

Jankowiak R, Ratsep M, Picorel R, Seibert M and Small GJ (1999) Excited states of the 5-chlorophyll Photosystem II reaction center. J Phys Chem B 103: 9759–9769

Jankowiak R, Tang D, Small GJ and Seibert M (1989) Transient and persistent hole burning of the reaction center of Photosystem II. J Phys Chem 93: 1649–1654

Johnston HG, Wang J, Ruffle S, Sayre RT and Gustafson TL (2000) Fluorescence decay kinetics of wild type and D2-H177N mutant Photosystem II reaction centers isolated from $Chlamydomonas$ $reinhardtii$. J Phys Chem B 104: 4777–4781

Kirmaier C and Holten D (1993) Electron transfer and charge recombination reactions in wild-type and mutant bacterial reaction centers. In: Deisenhofer J and Norris JR (eds) The Photosynthetic Reaction Center, Vol II, pp 49–70. Academic Press, San Diego, California

Knapp EW, Fischer SF, Zinth W, Sander M, Kaiser W, Deisenhofer J and Michel H (1985) Analysis of optical spectra from single crystals of $Rhodopseudomonas$ $viridis$ reaction centers. Proc Natl Acad Sci USA 82: 8463–8467

Kobayashi M, Maeda H, Watanabe T, Nakane H and Satoh K (1990) Chlorophyll a and β-carotene content in the D1/D2/cytochrome b-559 reaction center complex from spinach. FEBS Lett 260: 138–140

Konermann L and Holzwarth AR (1996) Analysis of the absorption spectrum of Photosystem II reaction centers: temperature dependence, pigment assignment, and inhomogeneous broadening. Biochemistry 35: 829–842

Konermann L, Gatzen G and Holzwarth AR (1997a) Primary process and structure of the Photosystem II reaction center. 5. Modeling of the fluorescence kinetics of the D_1–D_2-cyt-b_{559} complex at 77 K. J Phys Chem B 101: 2933–2944

Konermann L, Yruela I and Holzwarth AR (1997b) Pigment assignment in the absorption spectrum of the Photosystem II reaction center by site-selection fluorescence spectroscopy. Biochemistry 36: 7498–7502

Kumazaki S, Joseph DM, Crystall B, Tachibana Y, Durrant JR, Barber J, Porter G, Yoshihara K and Klug DR (1995) Experimental observation of multiple trapping/charge separation steps in the isolated PS II reaction centre. In: Mathis P (ed) Photosynthesis: From Light to Biosphere, Vol I, pp 883–886. Kluwer Academic Publishers, Dordrecht, The Netherlands

Kwa SLS, Newell WR, van Grondelle R and Dekker JP (1992) The reaction center of Photosystem II studied with polarized fluorescence spectroscopy. Biochim Biophys Acta 1099: 193–202

Kwa SLS, Eijckelhoff C, van Grondelle R and Dekker JP (1994a) Site-selection spectroscopy of the reaction center complex of Photosystem II. 1. Triplet-minus-singlet absorption difference: search for a second exciton band of P680. J Phys Chem 98: 7702–7711

Kwa SLS, Tilly NT, Eijckelhoff C, van Grondelle R and Dekker JP (1994b) Site-selection spectroscopy of the reaction center complex of Photosystem II. 2. Identification of the fluorescing species at 4 K. J Phys Chem 98: 7712–7716

Merry SAP, Kumazaki S, Tachibana Y, Joseph DM, Porter G, Yoshihara K, Barber J, Durrant JR and Klug DR (1996) Subpicosecond equilibration of excitation energy in isolated Photosystem II reaction centers revisited: time-dependent anisotropy. J Phys Chem 100: 10469–10478

Merry SAP, Nixon PJ, Barter LMC, Schilstra M, Porter G, Barber J, Durrant JR and Klug DR (1998) Modulation of quantum yield of primary radical pair formation in Photosystem II by site-directed mutagenesis affecting radical cations and anions. Biochemistry 37: 17439–17447

Mimuro M, Tomo T, Nishimura Y, Yamazaki I and Satoh K (1995) Identification of a photochemically inactive pheophytin molecule in the spinach D1–D2-cyt b559 complex. Biochim Biophys Acta 1232: 81–88

Muller Mg, Hucke M, Reus M and Holzwarth AR (1996) Primary processes and structure of the Photosystem II reaction center. 4. Low-intensity femtosecond transient absorption spectra of D1–D2-cyt-b559 reaction centers. J Phys Chem 100: 9527–9536

Nogi T, Fathir I, Kobayashi M, Nozawa T and Miki K (2000) Crystal structures of photosynthetic reaction center and high-potential iron–sulfur protein from $Thermochromatium$ $tepidum$: thermostability and electron transfer. Proc Natl Acad Sci USA 97: 13561–13566

Noguchi T, Tomo T and Inoue Y (1998) Fourier transform infrared study of the cation radical of P680 in the Photosystem II reaction center: evidence for charge delocalization on the chlorophyll dimer. Biochemistry 37: 13614–13625

Ogrodnik A, Keupp W, Volk M, Aumeier G and Michel-Beyerle ME (1994) Inhomogeneity of radical pair energies in photosynthetic reaction centers revealed by differences in recombination dynamics of P+H– when detected in delayed emission and in absorption. J Phys Chem 98: 3432–3439

Otte SCM, van der Vos R and van Gorkom HJ (1992) Steady state spectroscopy at 6 K of the isolated Photosystem II reac-

tion centre: analysis of the red absorption band. J Photochem Photobiol B Biol 15: 5–14

Peterman EJG, van Amerongen H, van Grondelle R and Dekker JP (1998) The nature of the excited state of the reaction center of Photosystem II of green plants: a high-resolution fluorescence spectroscopy study. Proc Natl Acad Sci USA 95: 6128–6133

Prokhorenko VI and Holzwarth AR (2000) Primary processes and structure of the Photosystem II reaction center: a photon echo study. J Phys Chem B 104: 11563–11578

Reddy NRS, Kolaczkowski SV and Small GJ (1993) Nonphotochemical hole burning of the reaction center of *Rhodopsuedomonas viridis*. J Phys Chem 97: 6934–6940

Roelofs TA, Gilbert M, Shuvalov VA and Holzwarth AR (1991) Picosecond fluorescence kinetics of the D1–D2-cyt-*b*-559 Photosystem II reaction center complex. Energy transfer and primary charge separation processes. Biochim Biophys Acta 1060: 237–244

Rutherford AW (1986) How close is the analogy between the reaction center of Photosystem II and that of purple bacteria. Biochem Soc Trans 14: 15–17

Satoh K (1993) Isolation and properties of the Photosystem II reaction center. In: Deisenhofer J and Norris JR (eds) The Photosynthetic Reaction Center, Vol I, pp 289–318. Academic Press, San Diego, California

Schelvis JPM, van Noort PI, Aartsma TJ and van Gorkom HJ (1994) Energy transfer, charge separation and pigment arrangement in the reaction center of Photosystem II. Biochim Biophys Acta 1184: 242–250

Scherer POJ and Fischer SF (1987) Model studies to low-temperature optical transitions of photosynthetic reaction centers. II. *Rhodobacter sphaeroides* and *Chloroflexus aurantiacus*. Biochim Biophys Acta 891: 157–164

Scherz A and Rosenbach-Belkin V (1988) The spectral properties of chlorophyll and bacteriochlorophyll dimers; a comparative study. In: Breton J and Vermiglio A (eds) The Photosynthetic Bacterial Reaction Center, pp 295–306. Plenum Press, New York

Seibert M (1993) Biochemical, biophysical and structural characterization of the isolated Photosystem II reaction center complex. In: Deisenhoffer J and Norris JR (eds) The Photosynthetic Reaction Center, vol I, pp 319–356. Academic Press, San Diego, California

Shipman LL (1977) Oscillator and dipole strengths for chlorophyll and related molecules. Photochem Photobiol 26: 287–292

Shkuropatov AY, Khatypov RA, Volshchukova TS, Shkuropatova VA, Owens TG and Shuvalov VA (1997) Spectral and photochemical properties of borohydride-treated D1–D2-cytochrome *b*-559 complex of Photosystem II. FEBS Lett 420: 171–174

Stewart DH, Nixon PJ, Diner BA and Brudvig GW (2000) Assignment of the Q_y absorbance bands of Photosystem II chromophores by low-temperature optical spectroscopy of wild-type and mutant reaction centers. Biochemistry 39: 14583–14594

Svensson B, Etchebest C, Tuffery P, van Kan P, Smith J and Styring S (1996) A model for the Photosystem II reaction center core including the structure of the primary donor P-680. Biochemistry 35: 14486–14502

Tang D, Jankowiak R, Seibert M, Yocum CF and Small GJ (1990) Excited-state structure and energy-transfer dynamics of two different preparations of the reaction center of Photosystem II: a hole-burning study. J Phys Chem 94: 6519–6522

Tang D, Jankowiak R, Seibert M and Small GJ (1991) Effects of detergent on the excited state structure and relaxation dynamics of the Photosystem II reaction center: a high resolution hole burning study. Photosynth Res 27: 19–29

Vacha F, Joseph DM, Durrant JR, Telfer A, Klug DR, Porter G and Barber J (1995) Photochemistry and spectroscopy of a five-chlorophyll reaction center of Photosystem II isolated by using a Cu affinity column. Proc Natl Acad Sci USA 92: 2929–2933

van Amerongen H, Valkunas L and van Grondelle R (2000) Photosynthetic Excitons, World Scientific, Singapore

van Brederode ME and van Grondelle R (1999) New and unexpected routes for ultrafast electron transfer in photosynthetic reaction centers. FEBS Lett 455: 1–7

van der Vos R, van Leeuwen PJ, Braun P and Hoff AJ (1992) Analysis of the optical absorbance spectra of D1–D2-cytochrome *b*-559 complexes by absorbance-detected magnetic resonance. Structural properties of P680. Biochim Biophys Acta 1140: 184–198

van Gorkom HJ (1995) Current questions on optical properties and energy transfer in the reaction center of Photosystem II. In: Mathis P (ed) Photosynthesis: From Light to Biosphere, Vol I, pp 437–442. Kluwer Academic Publishers, Dordrecht, The Netherlands

van Gorkom HJ and Schelvis JPM (1993) Kok's oxygen clock: What makes it tick? The structure of P680 and consequences of its oxidizing power. Photosynth Res 38: 297–301

van Grondelle R, Dekker JP, Gillbro T and Sundstrom V (1994) Energy transfer and trapping in photosynthesis. Biochim Biophys Acta 1187: 1–65

van Kan PJM, Otte SCM, Kleinherenbrink FAM, Nieveen MC, Aartsma TJ and van Gorkom HJ (1990) Time-resolved spectroscopy at 10 K of the Photosystem II reaction center; deconvolution of the red absorption band. Biochim Biophys Acta 1020: 146–152

van Mieghem FJE, Satoh K and Rutherford AW (1991) A chlorophyll tilted 30 degrees relative to the membrane in the Photosystem II reaction center. Biochim Biophys Acta 1058: 379–385

Vasil'ev S and Bruce D (2000) Picosecond time-resolved fluorescence studies on excitation energy transfer in a Histidine 117 mutant of the D2 protein of Photosystem II in *Synechocystis* 6803. Biochemistry 39: 14211–14218

Vasil'ev S, Orth P, Zouni A, Owens TG and Bruce D (2001) Excited state dynamics in PS II: insights from the X-ray crystal structure. Proc Natl Acad Sci USA 98: 8602–8607

Volk M, Gilbert M, Rousseau G, Richter M, Ogrodnik A and Michel-Beyerle M-E (1993) Similarity of primary radical pair recombination in Photosystem II and bacterial reaction centers. FEBS Lett 336: 357–362

Yang M and Fleming GR (2000) Third-order nonlinear optical response and energy transfer in static disordered systems. J Chem Phys 113: 2823–2840

Yeates TO, Komiya H, Chirino A, Rees DC, Allen JP and Feher G (1988) Structure of the reaction center from *Rhodobacter-sphaeroides* R-26 and 2.4.1-protein cofactor (bacteriochlorophyll, bacteriopheophytin, and carotenoid) interactions. 4. Proc Natl Acad Sci USA 85: 7993–7997

Yruela I, Tomas R, Alfonso M and Picorel R (1999) Effect of the pH on the absorption spectrum of the isolated D1–D2-cytochrome *b* 559 complex of Photosystem II. J Photochem Photobiol B Biol 50: 129–136

Zhang LY and Friesner RA (1998) *Ab initio* calculation of electronic coupling in the photosynthetic reaction center. Proc Natl Acad Sci USA 95: 13603–13605

Zouni A, Witt H-T, Kern J, Fromme P, Krauss N, Saenger W and Orth P (2001) Crystal structure of Photosystem II from *Synechococcus elongatus* at 3.8 Angstrom resolution. Nature 409: 739–743